

# Molecular Orbitals of the Oxocarbons $(\text{CO})_n$ , $n = 2-6$ . Why Does $(\text{CO})_4$ Have a Triplet Ground State?

Xiaoguang Bao,<sup>†</sup> Xin Zhou,<sup>†</sup> Charity Flener Lovitt,<sup>†</sup> Amruth Venkatraman,<sup>†</sup> David A. Hrovat,<sup>†</sup> Rolf Gleiter,<sup>‡</sup> Roald Hoffmann,<sup>\*,§</sup> and Weston Thatcher Borden<sup>\*,†</sup>

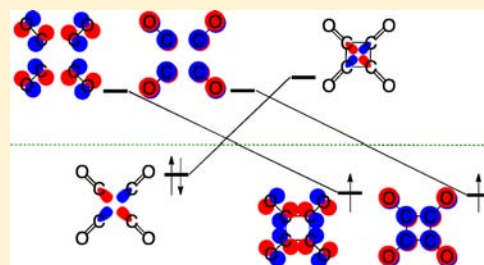
<sup>†</sup>Department of Chemistry and the Center for Advanced Scientific Computing and Modeling, University of North Texas, 1155 Union Circle, No. 305070, Denton, Texas 76203-5070, United States

<sup>‡</sup>Organisch-Chemisches Institut der Universität Heidelberg Im Neuenheimer Feld 270, D-69120 Heidelberg, Germany

<sup>§</sup>Department of Chemistry and Chemical Biology, Cornell University, Baker Laboratory, Ithaca, New York 14853-1301, United States

## Supporting Information

**ABSTRACT:** Cyclobutane-1,2,3,4-tetrone has been both predicted and found to have a triplet ground state, in which a  $b_{2g}$   $\sigma$  MO and an  $a_{2u}$   $\pi$  MO are each singly occupied. The nearly identical energies of these two orbitals of  $(\text{CO})_4$  can be attributed to the fact that both of these MOs are formed from a bonding combination of C–O  $\pi^*$  orbitals in four CO molecules. The intrinsically stronger bonding between neighboring carbons in the  $b_{2g}$   $\sigma$  MO compared to the  $a_{2u}$   $\pi$  MO is balanced by the fact that the non-nearest-neighbor, C–C interactions in  $(\text{CO})_4$  are antibonding in  $b_{2g}$ , but bonding in  $a_{2u}$ . Crossing between an antibonding,  $b_{1g}$  combination of carbon lone-pair orbitals in four CO molecules and the  $b_{2g}$  and  $a_{2u}$  bonding combinations of  $\pi^*$

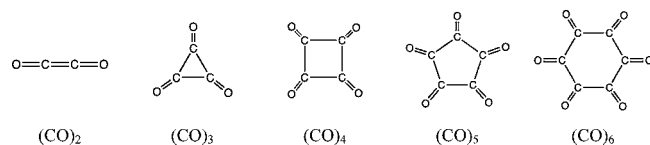


MOs is responsible for the occupation of the  $b_{2g}$  and  $a_{2u}$  MOs in  $(\text{CO})_4$ . A similar orbital crossing occurs on going from two CO molecules to  $(\text{CO})_2$ , and this crossing is responsible for the triplet ground state that is predicted for  $(\text{CO})_2$ . However, such an orbital crossing does not occur on formation of  $(\text{CO})_{2n+1}$  from  $2n + 1$  CO molecules, which is why  $(\text{CO})_3$  and  $(\text{CO})_5$  are both calculated to have singlet ground states. Orbital crossings, involving an antibonding,  $b_1$ , combination of lone-pair MOs, occur in forming all  $(\text{CO})_{2n}$  molecules from  $2n$  CO molecules. Nevertheless,  $(\text{CO})_6$  is predicted to have a singlet ground state, in which the  $b_{2u}$   $\sigma$  MO is doubly occupied and the  $a_{2u}$   $\pi$  MO is left empty. The main reason for the difference between the ground states of  $(\text{CO})_4$  and  $(\text{CO})_6$  is that interactions between  $2p$  AOs on non-nearest-neighbor carbons, which stabilize the  $a_{2u}$   $\pi$  MO in  $(\text{CO})_4$ , are much weaker in  $(\text{CO})_6$ , due to the much larger distances between non-nearest-neighbor carbons in  $(\text{CO})_6$  than in  $(\text{CO})_4$ .

## INTRODUCTION

Oxocarbons,  $(\text{CO})_n$  can be regarded as cyclic oligomers of carbon monoxide.<sup>1</sup> The dianions of oxocarbons, such as acetylenediolate  $(\text{CO})_2^{2-}$ ,<sup>2</sup> deltate  $(\text{CO})_3^{2-}$ ,<sup>3</sup> squarate  $(\text{CO})_4^{2-}$ ,<sup>4</sup> croconate  $(\text{CO})_5^{2-}$ ,<sup>5</sup> and rhodizone  $(\text{CO})_6^{2-}$ ,<sup>6</sup> are well-known for their thermodynamic stability and have been studied extensively.<sup>7</sup>

Consider the neutral oxocarbons,  $(\text{CO})_n$ ,  $n = 2-6$ , which have two fewer  $\pi$  electrons. These molecules are shown below. For each, an unexceptional Lewis structure can be drawn, so one might expect that these will be “normal” molecules. Therefore, the most interesting question about the  $(\text{CO})_n$  oxocarbons might appear to be whether at least some of these molecules are endowed with a modicum of kinetic stability toward fragmentation to  $n$  molecules of CO.



However, as we will see in this paper, there is much, much more to learn about these molecules. Despite the unexceptional

Lewis structure that can be drawn for each  $(\text{CO})_n$  molecule, the electronic structures of these neutral oxocarbons have some real surprises in store for us.

What is known experimentally? Not surprisingly, neutral oxocarbons appear to be highly unstable, both thermodynamically and kinetically. For example, only trace amounts of cyclobutane-1,2,3,4-tetrone  $(\text{CO})_4$ , cyclopentane-1,2,3,4,5-pentone  $(\text{CO})_5$ , and cyclohexane-1,2,3,4,5,6-hexone  $(\text{CO})_6$  have been detectable by mass spectrometry.<sup>8a</sup> Formation of a short-lived cyclopropane-1,2,3-trione  $(\text{CO})_3$  intermediate was proposed in the reaction of oxygen atoms with carbon suboxide ( $\text{C}_3\text{O}_2$ ), but  $(\text{CO})_3$  itself was not observed directly.<sup>8b</sup> In fact, density functional theory (DFT) calculations predict that cyclopropane-1,2,3-trione is a mountaintop on the  $(\text{CO})_3$  potential energy surface,<sup>7b,c</sup> although some ab initio calculations do find that  $D_{3h}$   $(\text{CO})_3$  is a local energy minimum.<sup>9</sup>

$(\text{CO})_2$  and, more recently,  $(\text{CO})_4$  have been of particular interest to computational chemists, because  $(\text{CO})_2$  is predicted to have a triplet ground state<sup>10</sup> and, quite surprisingly,  $(\text{CO})_4$  is

Received: April 9, 2012

Published: June 11, 2012

also calculated to have a very low-lying triplet state.<sup>11</sup> Performing calculations which are sufficiently reliable to be able to predict definitively the relative energies of the triplet and low-lying singlet states of  $(\text{CO})_4$  has proven to be unexpectedly challenging.<sup>11</sup>

In neutral  $(\text{CO})_4$ , two electrons must be distributed between the  $b_{2g}$  and  $a_{2u}$  MOs. Perhaps the most convincing argument for a triplet ground state for  $(\text{CO})_4$  comes from calculations which find that  ${}^2B_{2g}$  and  ${}^2A_{2u}$  states of both the  $(\text{CO})_4$  radical cation and  $(\text{CO})_4$  radical anion are very close in energy.<sup>12</sup> Since the  ${}^2B_{2g}$  and  ${}^2A_{2u}$  states of both  $(\text{CO})_4^{\bullet+}$  and  $(\text{CO})_4^{\bullet-}$  differ by whether the unpaired electron occupies a  $b_{2g}$  or  $a_{2u}$  MO, these two MOs of  $(\text{CO})_4$  must also have nearly the same energies. In addition to being nearly degenerate in energy, these orbitals are non-disjoint,<sup>13</sup> so Hund's rule<sup>14</sup> should apply to  $(\text{CO})_4$ . Therefore, despite the unexceptional, closed-shell, Lewis structure that can be drawn for  $(\text{CO})_4$ , the triplet has unequivocally been predicted to be the ground state.<sup>12</sup>

This theoretical prediction has very recently been confirmed experimentally.<sup>15</sup> Wang and co-workers generated the radical anion of  $(\text{CO})_4$  and measured its negative ion photoelectron spectrum. The triplet state was found to lie below the lowest singlet state of  $(\text{CO})_4$  by 1.5 kcal/mol, in good agreement with the results of (U)CCSD(T) calculations.<sup>11b-d</sup>

The level ordering in  $(\text{CO})_4$ —that the  $b_{2g}$   $\sigma$  and  $a_{2u}$   $\pi$  MOs of  $(\text{CO})_4$  are nearly degenerate in energy—turns out to contain the key to the peculiarities of the electronic structures of the neutral oxocarbons. In this paper we show that the reason for near degeneracy of this pair of MOs in  $(\text{CO})_4$  is closely related to the symmetry-enforced degeneracy of the  $\pi_u$  MOs in  $(\text{CO})_2$ . We also explain why, unlike the case in  $(\text{CO})_2$  and  $(\text{CO})_4$ ,  $(\text{CO})_{2n+1}$  oxocarbons, such as  $(\text{CO})_3$  and  $(\text{CO})_5$ , have closed-shell, singlet ground states. Finally, we describe the reasons why  $(\text{CO})_6$ , unlike the  $(\text{CO})_{2n}$  oxocarbons with  $n = 1$  and  $2$ , is also predicted to have a singlet ground state.

## ■ COMPUTATIONAL METHODOLOGY

$D_{nh}$  geometries ( $n = 2-6$ ) for the neutral  $(\text{CO})_n$  oxocarbons were optimized with B3LYP DFT calculations.<sup>16</sup> Unrestricted (U)B3LYP calculations were performed on triplets and monoradicals. Vibrational frequency analyses were performed to ensure that the optimized  $D_{nh}$  structures corresponded to local minima, and the calculated frequencies yielded the zero-point vibrational energy (ZPVE) corrections. Single-point coupled-cluster calculations at the (U)CCSD(T) level<sup>19</sup> were performed at the (U)B3LYP-optimized geometries. Except where noted, the 6-311+G(2df) basis set<sup>20</sup> was used for all of our calculations, which were carried out with the Gaussian 09 suite of programs.<sup>21</sup>

## ■ RESULTS AND DISCUSSION

**MOs of  $(\text{CO})_4$ .** We enter the essential problem in the electronic structure of  $(\text{CO})_n$  oxocarbons through  $(\text{CO})_4$ . The two, nearly degenerate, MOs of  $(\text{CO})_4$ , each of which is singly occupied in the triplet ground state, are depicted in Figure 1.<sup>11,12</sup> The MOs look very different, and they have different symmetries. The  $b_{2g}$  MO is a  $\sigma$  orbital, and the  $a_{2u}$  MO is a  $\pi$  orbital.

However, these two MOs do share some features. For example, they are each comprised largely of 2p AOs on carbon and oxygen. In both MOs the 2p AOs on carbon are in-phase with each other, but out-of-phase with the 2p AOs on the oxygen atom to which each carbon is attached.

In fact, Figure 2 shows that the  $b_{2g}$  and  $a_{2u}$  MOs of  $(\text{CO})_4$  share a common origin in the  $\pi$  MOs of carbon monoxide, and that is why these MOs of  $(\text{CO})_4$  are nearly degenerate in energy.

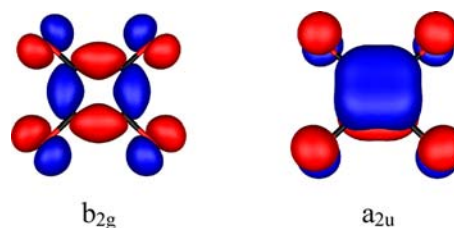


**Figure 1.** The two MOs that are singly occupied in the triplet ground state of  $(\text{CO})_4$ .

The MOs are each formed by the in-phase overlap of one of the degenerate pair of the  $\pi^*$  MOs of four CO molecules. The  $b_{2g}$  MO is formed from the CO  $\pi^*$  MOs that lie in the molecular plane of  $(\text{CO})_4$ , and the  $a_{2u}$  MO is formed from the CO  $\pi^*$  MOs that have a node in the plane of the molecule.

Although the  $b_{2g}$  and  $a_{2u}$  MOs of  $(\text{CO})_4$  both have their parentage in the degenerate pairs of  $\pi^*$  MOs in four isolated CO molecules, the nearly equal energies of the  $b_{2g}$  and  $a_{2u}$  MOs of  $(\text{CO})_4$  are, nevertheless, surprising. One might have expected that the  $\sigma$  overlaps of the 2p AOs on adjacent carbons in the  $b_{2g}$  MO would have created stronger C–C bonding than the  $\pi$  overlaps that are present in the  $a_{2u}$  MO. However, Figures 1 and 2 both show that there is a compensating factor.

In the  $a_{2u}$   $\pi$  MO of  $(\text{CO})_4$  the cross-ring  $\pi$  overlaps between the 2p AOs on C1 and C3 and on C2 and C4 are bonding. In contrast, the different topologies of orbital interactions in creating  $\sigma$  and  $\pi$  bonding overlaps between nearest-neighbor 2p AOs result in the cross-ring  $\sigma$  overlaps between the 2p AOs on C1 and C3 and on C2 and C4 being antibonding in the  $b_{2g}$  MO. It is presumably a near cancellation between stronger nearest-neighbor  $\sigma$  bonding in the  $b_{2g}$  MO and stronger non-nearest-neighbor  $\pi$  bonding in the  $a_{2u}$  MO that results in the nearly degenerate energies of these two MOs in  $(\text{CO})_4$ .<sup>12</sup> We will return to this subject in a subsequent section.

Why are combinations of the antibonding,  $\pi^*$  orbitals of four CO molecules filled in the triplet state of the tetramer? The diagram in Figure 2 also provides the answer to this question. As shown in Figure 2, the  $b_{1g}$  combination of lone-pair orbitals on the carbons of four CO molecules (the most antibonding of the four lone-pair combinations; the other three are not shown) becomes a highly antibonding, unfilled MO in  $(\text{CO})_4$ . The pair of electrons in the  $b_{1g}$  combination of carbon lone-pair orbitals in four CO molecules are removed from this MO in  $(\text{CO})_4$ , and the electrons are distributed between the nearly degenerate  $b_{2g}$   $\sigma$  and  $a_{2u}$   $\pi$  MOs of  $(\text{CO})_4$ . The possibility, which turns into a reality, of a high-spin ground state for the molecule is thus created.

Now let us consider the diagram in Figure 2 as a real orbital correlation diagram for a chemical reaction, the fragmentation of  $(\text{CO})_4$  into four CO molecules. Because there are crossings between orbitals that are filled in the reactant and empty in the product and vice versa, this hypothetical reaction, the thermodynamically favorable decomposition of  $(\text{CO})_4$  to four CO molecules, is forbidden to be concerted by orbital symmetry.<sup>22</sup>

To compute the barrier to concerted breaking of all four ring bonds in  $(\text{CO})_4$ , starting from the singlet state in which the  $b_{2g}$   $\sigma$  MO is doubly occupied, we performed (8/8)CASSCF/6-31G(d)<sup>23</sup> and CASPT2/6-31G(d) calculations.<sup>24,25</sup> At the CASSCF level of theory, the reaction  $(\text{CO})_4 \rightarrow 4\text{CO}$  is exothermic by 71.4 kcal/mol, but concerted breaking of all four ring bonds has a barrier height of 93.8 kcal/mol. The CASPT2 values for the exothermicity and barrier height are, respectively,

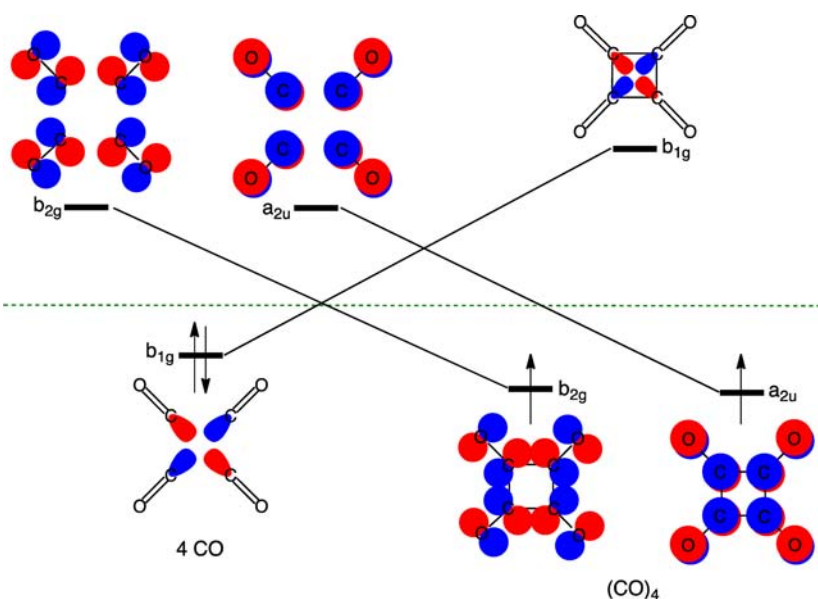


**Figure 2.** Diagram showing how the  $b_{1g}$ ,  $b_{2g}$ , and  $a_{2u}$  MOs of  $(\text{CO})_4$  are formed from symmetry combination of the orbitals of four CO molecules. The orbitals below the dotted line—the  $b_{1g}$  MO in four CO molecules and the  $b_{2g}$  and  $a_{2u}$  MOs in triplet  $(\text{CO})_4$ —are filled. Just the frontier orbitals are shown. There are three other combinations of CO lone pairs, which are all filled in  $(\text{CO})_4$ , and six other combinations of CO  $\pi^*$  parentage, which are all empty in  $(\text{CO})_4$ .

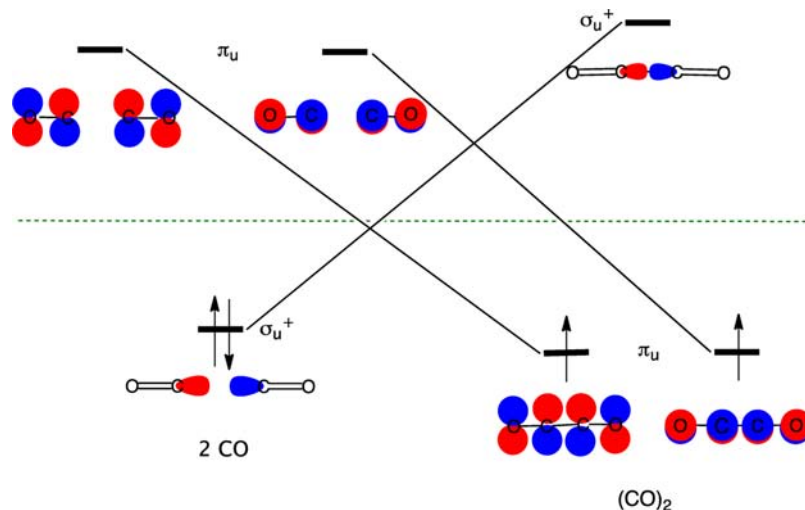


**Figure 3.** Diagram showing how the  $\sigma_u$  and  $\pi_u$  MOs of  $(\text{CO})_2$  are formed from symmetry combinations of the orbitals of two CO molecules. The orbitals below the dotted line— $\sigma_u^+$  in two CO molecules and  $\pi_u$  in  $(\text{CO})_2$ —are filled.

55.3 and 92.1 kcal/mol.<sup>26</sup> Given the very large exothermicity, the molecule will find ways to fragment in stepwise fashion.<sup>27</sup>

**Similarity between the Electronic Structures of  $(\text{CO})_2$  and  $(\text{CO})_4$ .** A glance back at previous work on  $(\text{CO})_2$  shows that there is a close analogy between the electronic structures of  $(\text{CO})_2$  and  $(\text{CO})_4$ . Figure 3 shows the construction of the corresponding MOs for the CO dimer. In the formation of  $(\text{CO})_2$  from two CO molecules, just as in the formation of  $(\text{CO})_4$  from four CO molecules, a pair of electrons must be removed from an out-of-phase combination of carbon lone-pair orbitals. In both molecules this pair of electrons can occupy the in-phase combinations of either of two sets of C–O  $\pi^*$  orbitals. However, unlike the case in  $(\text{CO})_4$ , in  $(\text{CO})_2$  symmetry makes these two sets of  $\pi^*$  orbitals exactly degenerate in energy.

In  $(\text{CO})_4$ , because the  $b_{2g}$  and  $a_{2u}$  combinations of C–O  $\pi^*$  MOs are not degenerate by symmetry, calculations are necessary to predict the relative energies of the triplet and lowest singlet

states. In contrast, without performing any calculations, the symmetry-mandated degeneracy of the highest occupied pair of orbitals in  $(\text{CO})_2$  and their nondisjoint nature<sup>14</sup> allow Hund's rule<sup>15</sup> to be used to predict unequivocally that the ground state of  $(\text{CO})_2$  is a triplet. Previous calculations have, indeed, confirmed the prediction of a triplet ground state for  $(\text{CO})_2$ .<sup>10</sup> (U)CCSD(T)<sup>10k</sup> and MR-CI calculations<sup>10m</sup> both place the triplet state of  $(\text{CO})_2$  slightly more than 9 kcal/mol below the lowest singlet state.

**MOs of  $(\text{CO})_3$ .** Do the other oxocarbons behave like  $(\text{CO})_2$  and  $(\text{CO})_4$  and have triplet ground states? As we will see in this section, the answer for  $(\text{CO})_3$  is an unequivocal no, because the electronic structure of this oxocarbon is very different from those of  $(\text{CO})_2$  and  $(\text{CO})_4$ .

The carbon lone-pair orbitals on three CO molecules span the  $a_1'$  and degenerate  $e'$  representations of the  $D_{3h}$  point group. The  $a_1'$  combination is nodeless, but as shown on the right-hand

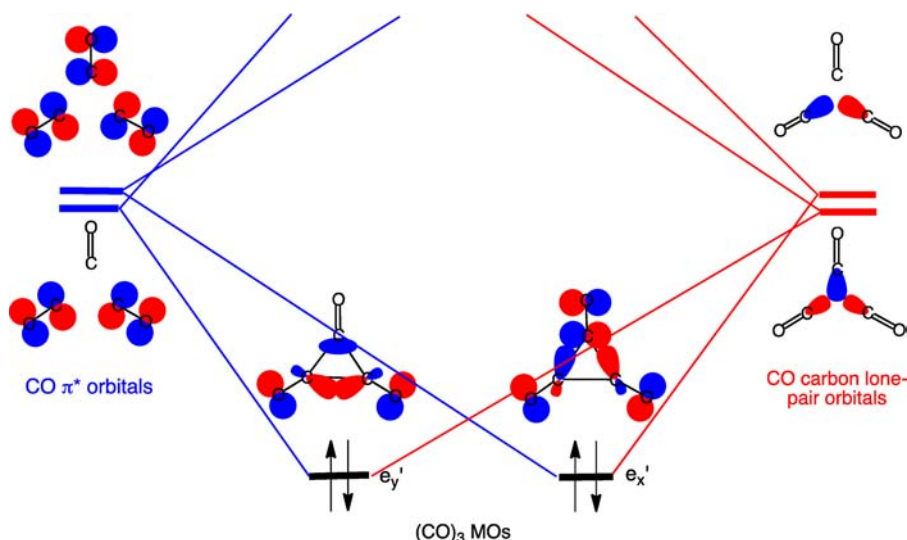


**Figure 4.** Orbital interaction diagram showing schematically how the  $e'$  combinations of the carbon lone-pair orbitals of three CO molecules are stabilized by mixing with the  $e'$  combinations of the in-plane  $\pi^*$  orbitals in forming the degenerate  $e'$  MOs of  $(\text{CO})_3$ . The relative energies of the  $e'$  combinations of lone-pair and in-plane  $\pi^*$  MOs are depicted as being almost the same, but the relative energies of these two sets of orbitals actually change with the distance between the three CO molecules.

side of the orbital interaction diagram in Figure 4, the  $e'$  combinations of the lone-pair orbitals each have one node. Therefore, in the absence of any other orbital mixing, the antibonding interactions between the carbon lone pairs in the  $e'$  MOs of  $(\text{CO})_3$  would cause these orbitals to be very high in energy. This is, of course, what happens in the  $b_{1g}$  MO of  $(\text{CO})_4$  (Figure 2) and in the  $\sigma_u^+$  MO of  $(\text{CO})_2$  (Figure 3).

However, Figure 4 shows that, unlike the  $b_{1g}$  MO of  $(\text{CO})_4$  and the  $\sigma_u^+$  MO of  $(\text{CO})_2$ , the  $e'$  carbon lone-pair orbitals of  $(\text{CO})_3$  are stabilized by mixing with another  $e'$  combination, derived from the formally empty, in-plane,  $\pi^*$  orbitals of the three CO molecules. The latter pair of orbitals has  $\sigma$  bonding interactions between the COs. The mixing of the two sets of  $e'$  orbitals results in the lower energy  $e'$  combinations, shown in the middle of Figure 4. These MOs, which are occupied in  $(\text{CO})_3$ , resemble the bonding  $e'$  ring orbitals of cyclopropane,<sup>28</sup> albeit with an admixture of the 2p lone-pair AOs on the three oxygens that is C–O antibonding.

As a result of the stabilization of the  $e'$  combinations of the carbon lone-pair orbitals by mixing with the in-plane C–O  $\pi^*$  orbitals, the  $e'$  pair of filled MOs on three CO molecules correlates with the filled,  $e'$  ring orbitals of  $D_{3h}$   $(\text{CO})_3$ . This correlation between the filled,  $e'$ , lone-pair MOs of three CO molecules and the filled,  $e'$  MOs of  $(\text{CO})_3$  is shown in Figure 5.

**Singlet–Triplet Splitting in  $(\text{CO})_3$  and the Fragmentation of Singlet  $(\text{CO})_3$  to Three CO Molecules.** Comparison of the diagram for formation of  $(\text{CO})_3$  from three CO molecules in Figure 5 with those for formation of  $(\text{CO})_4$  in Figure 2 and  $(\text{CO})_2$  in Figure 3 strongly suggests that, unlike  $(\text{CO})_2$  or  $(\text{CO})_4$ ,  $(\text{CO})_3$  is likely to have a closed-shell  $^1A_1'$  ground state. In  $(\text{CO})_2$  and  $(\text{CO})_4$  a total of two electrons must be placed into a pair of degenerate or nearly degenerate highest occupied molecular orbitals (HOMOs). In contrast, in  $(\text{CO})_3$  the degenerate  $e'$   $\sigma$  HOMOs are occupied by a total of four electrons, and the  $a_2''$   $\pi$  lowest unoccupied molecular orbital (LUMO) lies significantly higher in energy.<sup>29</sup>

Indeed, at the optimized  $D_{3h}$  geometries of singlet and triplet  $(\text{CO})_3$ , the energy difference between the closed-shell,  $^1A_1'$  singlet state and the triplet state is  $-13.9$  kcal/mol with (U)B3LYP/6-311+G(2df) calculations and  $-26.5$  kcal/mol with

(U)CCSD(T)/6-311+G(2df) calculations. The negative signs are meant to indicate that the singlet is computed to be lower in energy than the triplet by both types of calculations.

The results of these calculations on  $(\text{CO})_3$  can be compared with the results of our (U)B3LYP/6-311+G(2df) and (U)CCSD(T)/6-311+G(2df) calculations on  $(\text{CO})_4$ . The  $^3B_{1u}$  state of  $(\text{CO})_4$  is computed to lie lower in energy than the closed-shell,  $^1A_{1g}$  state that has eight  $\pi$  electrons by 14.0 kcal/mol with (U)B3LYP and by 2.4 kcal/mol with (U)CCSD(T).<sup>30</sup> Thus, our (U)B3LYP and (U)CCSD(T) results both indicate that the energy of the closed-shell singlet state is lower relative to that of the triplet state by 28–29 kcal/mol in  $(\text{CO})_3$  than in  $(\text{CO})_4$ .

However, this prediction that the ground state of  $D_{3h}$   $(\text{CO})_3$  is a singlet may be of only theoretical interest. This state is calculated by B3LYP to be a mountaintop and, after geometry distortion, to fragment to three CO molecules without a barrier.<sup>7b,9,31</sup> If  $(\text{CO})_3$  and the pathway for its fragmentation are both constrained to have  $D_{3h}$  symmetry, B3LYP finds  $\Delta E = -67.0$  kcal/mol for this reaction and a barrier of only 1.1 kcal/mol to concerted fragmentation of  $(\text{CO})_3$ .

The negligible barrier to concerted fragmentation of  $(\text{CO})_3$  to three CO molecules is, at least in part, a consequence of the smooth correlation between filled orbitals of reactant and product, shown in Figure 5. This reaction is allowed by orbital symmetry.<sup>22</sup>

**MOs of  $(\text{CO})_5$  and Other  $(\text{CO})_{2n+1}$  Molecules.** One might guess that the odd principal axis of symmetry in the  $D_{nh}$  point groups ( $m = 2n + 1$ ), to which planar  $(\text{CO})_3$ ,  $(\text{CO})_5$ , and other planar  $(\text{CO})_{2n+1}$  oxocarbons belong, would confer similar electronic structures on these molecules, and this guess is correct. The patterns of the MOs formed from (a) the carbon lone pairs and (b) the in-plane  $\pi^*$  MOs of  $2n + 1$  CO molecules can be used, in conjunction with group theory, to create the orbital interaction diagram in Figure 6, which proves this point.

The cyclic array of the  $2n + 1$  carbon lone-pair orbitals in  $2n + 1$  CO molecules constitutes a Hückel array.<sup>33</sup> Therefore, as shown in Figure 6, the orbitals that are formed by interactions between the  $2n + 1$  lone-pair orbitals on carbon follow the familiar Hückel pattern of one nondegenerate MO being lowest in energy,

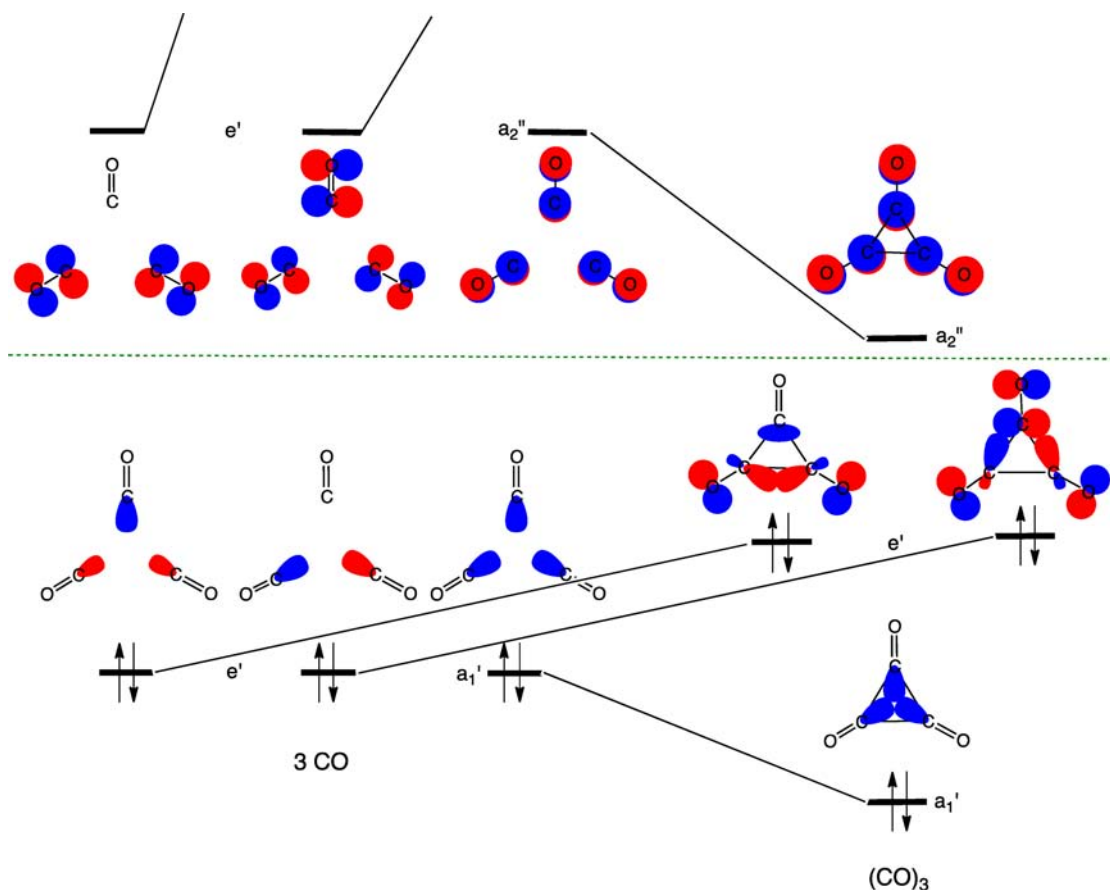


**Figure 5.** Orbital correlation diagram showing how the  $e'$ ,  $a_1'$ , and  $a_2''$  combinations of the lone-pair and  $\pi^*$  orbitals of three CO molecules correlate with the MOs of  $(\text{CO})_3$ . The orbitals below the dotted line are filled both in three CO molecules and in  $(\text{CO})_3$ .

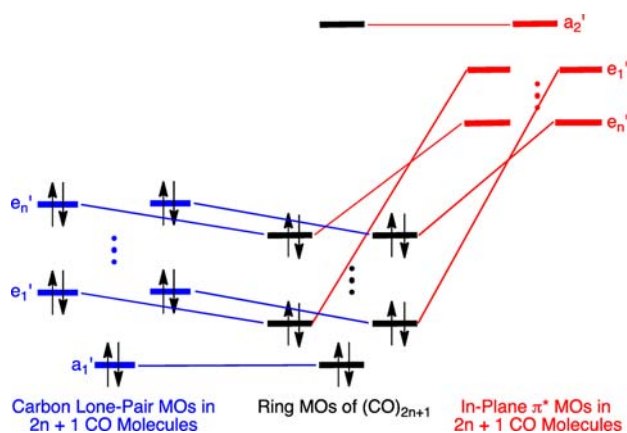


**Figure 6.** Orbital interaction diagram showing schematically the stabilization of the  $n$  degenerate pairs of carbon lone-pair MOs, which are filled in  $2n + 1$  CO molecules, by mixing with the  $n$  pairs of degenerate in-plane  $\pi^*$  MOs, which are empty in  $2n + 1$  CO molecules. This mixing between filled and empty MOs of  $2n + 1$  CO molecules forms all but one of the filled ring orbitals of  $(\text{CO})_{2n+1}$ . The carbon lone-pair orbitals are shown as being lower in energy than the in-plane  $\pi^*$  MOs. However, the relative energies of these two sets of orbitals actually change with the distance between the  $2n + 1$  CO molecules.

followed by  $n$  pairs of degenerate orbitals. The lowest energy, carbon lone-pair MO forms a nodeless, C–C, bonding MO, and the remaining  $2n$  carbon lone-pair MOs form  $n$  degenerate pairs of filled ring orbitals with 1, 2, ...,  $n$  nodes.

In contrast, the cyclic array of the in-plane  $\pi^*$  orbitals in  $2n + 1$  CO molecules constitutes a Möbius array. Therefore, as also indicated in Figure 6, the orbitals that are formed by interactions between the  $2n + 1$  in-plane  $\pi^*$  orbitals follow the familiar Möbius pattern,<sup>33</sup> with the lowest,  $n$ , in-plane  $\pi^*$  MOs occurring in degenerate pairs with 1, 2, ...,  $n$  nodes between carbons.

Mixing of the  $n$  filled pairs of degenerate, carbon, lone-pair orbitals with the  $n$  empty pairs of degenerate in-plane  $\pi^*$  MOs generates a total of  $n$  degenerate pairs of stabilized MOs. These degenerate pairs of MOs, along with the  $a_1'$  MO that results from the in-phase combination of carbon lone-pair AOs, comprise the filled ring MOs of  $(\text{CO})_{2n+1}$ . Thus, as in the specific case of  $(\text{CO})_3$ , the carbon lone-pair orbitals in  $2n + 1$  CO molecules correlate with the filled ring orbitals of  $(\text{CO})_{2n+1}$ .

The highest occupied pair of degenerate ring orbitals that are filled in  $(\text{CO})_5$  are shown in Figure 7. The large contribution of

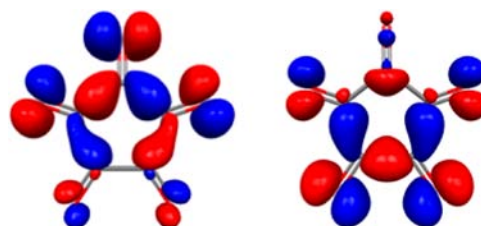


**Figure 7.** Degenerate pair of  $e_2'$  HOMOs of  $(\text{CO})_5$ .

the in-plane  $\pi^*$  MOs of five CO molecules to these  $e_2'$  MOs is evident in the antibonding interactions between the 2p AOs on

the oxygens and the AOs on the carbons that form these two degenerate, C–C bonding, ring MOs. The lone-pair orbitals on the five CO molecules make much smaller contributions to these  $e_2'$  MOs of  $(\text{CO})_5$ .

**Singlet–Triplet Splitting in  $(\text{CO})_5$  and the Fragmentation of Singlet  $(\text{CO})_5$  to Five CO Molecules.** The correlation of the filled MOs of  $2n + 1$  CO molecules with the filled MOs of  $(\text{CO})_{2n+1}$  has two consequences.

First, it means that, as in  $(\text{CO})_3$ , the degenerate pair of  $\sigma$  HOMOs of the ring are doubly occupied and that there is likely to be a significant energy difference between these  $\sigma$  MOs and the unoccupied,  $a_2''$   $\pi$  MO, in which all of the  $\pi^*$  CO orbitals are in-phase. Therefore, the ground state of all  $(\text{CO})_{2n+1}$  molecules should be a closed-shell singlet, as indeed the ground state is computed to be in planar  $(\text{CO})_5$ .

The (U)B3LYP value of the singlet–triplet energy separation in  $(\text{CO})_5$  is  $-10.7$  kcal/mol, and the (U)CCSD(T) value is  $-27.0$  kcal/mol, where the negative sign means that the singlet is computed to be lower in energy than the triplet. The negative ion photoelectron (NIPE) spectrum of  $(\text{CO})_5^{\bullet-}$  has recently been measured,<sup>34</sup> and as expected from the foregoing discussion of the MOs of  $(\text{CO})_5$  and from the results of our calculations, the ground state of  $(\text{CO})_5$  was found to be a singlet.

The second consequence of the correlation of the filled ring MOs of  $(\text{CO})_{2n+1}$  with the carbon lone-pair orbitals on  $2n + 1$  CO molecules is that the concerted fragmentation of  $(\text{CO})_{2n+1}$  to  $2n + 1$  CO molecules is allowed by orbital symmetry.<sup>22</sup> In the case of  $(\text{CO})_5$ , the concerted fragmentation, which preserves the  $D_{5h}$  symmetry of the equilibrium geometry, is computed by B3LYP to be exothermic by 25.4 kcal/mol and to have a barrier of 55.7 kcal/mol. The much larger barrier to concerted fragmentation of  $(\text{CO})_5$  than of  $(\text{CO})_3$  is, presumably, due to the ca. 40 kcal/mol lower exothermicity of the fragmentation of  $(\text{CO})_5$  and to the necessity of simultaneously breaking five, rather than three, C–C bonds in the concerted fragmentation reaction.

The  $D_{5h}$  energy maximum for the concerted fragmentation is found to have two pairs of degenerate vibrations with imaginary frequencies. Therefore, although concerted fragmentation of the  $(\text{CO})_5$  to five CO molecules is allowed by orbital symmetry, there must, in fact, be lower energy  $(\text{CO})_5$  fragmentation pathways, in which C–C bond breaking does not occur in a concerted fashion. We have not attempted to find the transition structures for stepwise breaking of the C–C bonds in  $(\text{CO})_5$ .

**MOs of  $(\text{CO})_6$  and Other  $(\text{CO})_{2n}$  Molecules.** In  $(\text{CO})_{2n}$ ,  $(\text{CO})_4$ ,  $(\text{CO})_6$ , and other  $(\text{CO})_{2n}$  molecules, the cyclic array of not only the lone-pair orbitals on carbon but also the in-plane  $\pi^*$  orbitals constitute a Hückel array.<sup>33</sup> Consequently, as shown in Figure 8, the lowest energy of each of these two sets of orbitals in  $(\text{CO})_{2n}$  is followed by  $n - 1$  degenerate pairs of orbitals of higher energy, which are followed by a nondegenerate, completely antibonding MO.

The highest energy, carbon, lone-pair MO of  $(\text{CO})_{2n}$  in Figure 8, like the  $b_{1g}$  MO of  $(\text{CO})_4$  in Figure 2, has all of the carbon lone-pair orbitals on adjacent carbons out-of-phase with each other. This  $b_1$  MO (whether it is  $b_{1g}$  or  $b_{1u}$  depends on whether  $n$  is even or odd) of  $(\text{CO})_{2n}$  has the wrong symmetry to mix with and, hence, be stabilized by any of the in-plane,  $\pi^*$  MOs of the  $2n$  CO molecules. Therefore, this  $b_{1g}/b_{1u}$  MO is highly C–C antibonding, and although it is filled in  $2n$  CO molecules, it is empty in  $(\text{CO})_{2n}$ .

The lowest energy, in-plane, C–O  $\pi^*$  MO of  $(\text{CO})_{2n}$  has the 2p AOs on all of the adjacent carbons in-phase. As in the  $b_{2g}$  MO of  $(\text{CO})_4$ , which is shown in Figures 1 and 2, the lowest energy,

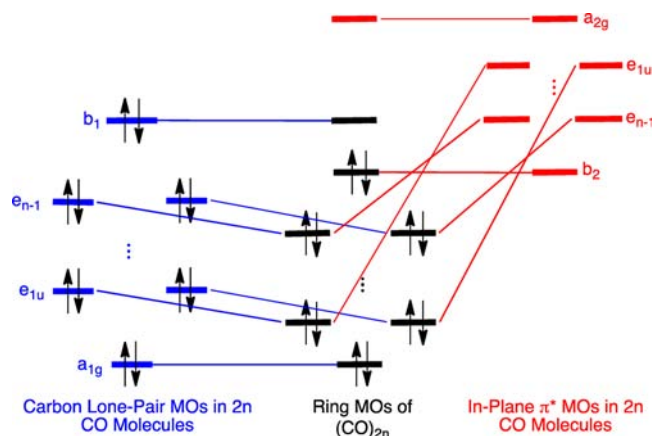


**Figure 8.** Orbital interaction diagram showing schematically the stabilization of the  $n - 1$  degenerate pairs of carbon lone-pair MOs, which are filled in  $2n$  CO molecules, by mixing with the  $n - 1$  degenerate pairs of degenerate, in-plane  $\pi^*$  MOs, which are empty in  $2n$  CO molecules. This mixing between filled and empty MOs of  $2n$  CO molecules forms all but two of the filled ring orbitals of  $(\text{CO})_{2n}$ . (Whether the  $e_{n-1}$ ,  $b_1$ , and  $b_2$  MOs are g or u depends on whether  $n$  is even or odd.) The  $b_2$ , in-plane,  $\pi^*$  MO, which is bonding between all the carbons, is depicted as being lower in energy than the  $b_1$ , carbon lone-pair MO, which is antibonding between all of the carbons. However, the relative energies of these two orbitals actually change with the distance between the  $2n$  CO molecules. The pair of electrons that occupy the  $b_1$  MO in  $2n$  isolated CO molecules are shown as occupying the  $b_2$  MO in singlet  $(\text{CO})_{2n}$ , but in the lowest triplet state, one of these two electrons occupies the  $a_{2u}$ , out-of-plane,  $\pi^*$  MO, which is not shown in this diagram.

in-plane, CO  $\pi^*$  MO of all  $(\text{CO})_{2n}$  molecules has the wrong symmetry to mix with any of the lone-pair orbitals on carbon.

As indicated in Figure 8, this  $b_2$  MO (whether it is  $b_{2g}$  or  $b_{2u}$  depends on whether  $n$  is even or odd) is empty in  $2n$  CO molecules, but it is doubly occupied in the lowest singlet state of  $(\text{CO})_{2n}$ . The pair of electrons that occupy the  $b_1$  carbon lone-pair MO in  $2n$  CO molecules occupy this  $b_2$  MO in the lowest singlet state of  $(\text{CO})_{2n}$ .<sup>29</sup> The change in which these two MOs are doubly occupied is due to a crossing between these MOs in forming  $(\text{CO})_{2n}$  from  $2n$  CO molecules.<sup>35</sup>

In the singlet state of  $(\text{CO})_{2n}$ , that is depicted in Figure 8, a pair of electrons occupy the  $b_2$ , C–C bonding combination of in-plane, CO,  $\pi^*$  MOs. However, in the triplet state one of these two electrons occupies the out-of-plane,  $a_{2u}$ , C–C bonding combination of CO  $\pi^*$  MOs. Whether the ground state of  $(\text{CO})_{2n}$  is a closed-shell singlet or a triplet depends on the relative energies of the in-plane ( $b_2$ ) and out-of-plane ( $a_{2u}$ ) C–C bonding combinations of the CO  $\pi^*$  MOs.

In  $(\text{CO})_2$  these two  $\pi^*$  MOs are degenerate by symmetry, so Hund's rule<sup>15</sup> predicts that the ground state of  $(\text{CO})_2$  should be a triplet.<sup>10</sup> In  $(\text{CO})_4$  the  $\sigma$  ( $b_{2g}$ ) and  $\pi$  ( $a_{2u}$ ) MOs, formed from the bonding combinations of the degenerate  $\pi^*$  MOs in four isolated CO molecules, are calculated to have nearly the same energy;<sup>12</sup> and this near degeneracy results in the ground state of  $(\text{CO})_4$  also being computed<sup>11b-d</sup> and found<sup>15</sup> to be a triplet. However, as described in the next section, our calculations find that, in  $(\text{CO})_6$ , the  $\sigma$  ( $b_{2u}$ ) C–C bonding MO is considerably lower in energy than the  $\pi$  ( $a_{2u}$ ) C–C bonding MO. Therefore, the ground state of  $(\text{CO})_6$  is expected to be a closed-shell singlet, in which, as shown schematically in Figure 9, the  $b_{2u}$   $\sigma$  MO is doubly occupied and the  $a_{2u}$   $\pi$  MO is left empty.<sup>29</sup>

**Singlet–Triplet Splitting in  $(\text{CO})_6$ .** The planar,  $D_{6h}$  geometry of singlet  $(\text{CO})_6$  is not an energy minimum,<sup>9</sup> but its

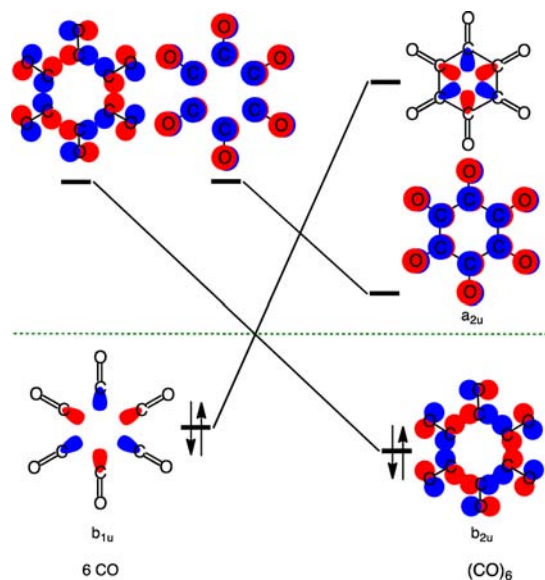


**Figure 9.** Orbital correlation diagram showing how the  $b_{1u}$ ,  $b_{2u}$ , and  $a_{2u}$  combinations of the orbitals of six CO molecules correlate with the MOs of  $(\text{CO})_6$ . [The correlations of the  $e_1'$  and  $e_2'$  combinations of the lone-pair orbitals on the carbons of six CO molecules with the filled  $e_1'$  and  $e_2'$  combinations of ring bonds in  $(\text{CO})_6$  are not shown.] The orbitals below the dotted line—the  $b_{1u}$  MO in six CO molecules and the  $b_{2u}$  MO in  $(\text{CO})_6$ —are filled. The significantly lower energy of the  $b_{2u}$   $\sigma$  MO of  $(\text{CO})_6$  compared to the  $a_{2u}$   $\pi$  MO is indicated schematically.

B3LYP energy is less than 1 kcal/mol higher than that of the  $D_{3d}$  chair, which is the lowest energy conformation. (See Table S1 in the Supporting Information.) Given the small energy difference between these two conformations of  $(\text{CO})_6$ , to facilitate comparisons with the results of the calculations on the  $D_{4h}$  geometry of  $(\text{CO})_4$ , the following discussion is based on calculations on planar  $(\text{CO})_6$  that were performed in  $D_{6h}$  symmetry.

Unlike the case in  $(\text{CO})_4$ , where  ${}^3B_{1u}$  is both predicted<sup>11b-d,12</sup> and found<sup>15</sup> to be the ground state, our calculations on  $(\text{CO})_6$  predict the ground state to be a closed-shell,  ${}^1A_{1g}$  state, with the  $b_{2u}$   $\sigma$  MO doubly occupied. Table 1 summarizes the (U)B3LYP and (U)CCSD(T) singlet–triplet energy differences in  $(\text{CO})_n$ ,  $n = 2–6$ . The  ${}^1A_{1g}$  state of  $(\text{CO})_6$  is computed to lie lower than the  ${}^3B_{2g}$  state by  $-9.5$  kcal/mol with (U)B3LYP/6-311+G(2df) and by  $-27.8$  kcal/mol with (U)CCSD(T)/6-311+G(2df).

The NIPE spectrum of  $(\text{CO})_6^{\bullet-}$  has recently been measured.<sup>34</sup> As predicted by our calculations, the ground state of  $(\text{CO})_6$  was found to be a singlet, which lies well below the lowest triplet state.

The reason that  $(\text{CO})_6$  is calculated to have a singlet ground state, in which the  $b_{2u}$   $\sigma$  MO is doubly occupied, is that this MO of  $(\text{CO})_6$  is considerably lower in energy than the  $a_{2u}$   $\pi^*$  MO. The energies of these two MOs can be compared by computing the two lowest ionization energies (IEs) of the  ${}^3B_{1g}$  state, in which one electron occupies the  $b_{2u}$  MO and one electron occupies the  $a_{2u}$  MO.<sup>12</sup> According to Koopmans' theorem,<sup>37</sup> the energy difference between removing the electron from the  $b_{2u}$  MO and from the  $a_{2u}$  MO in the  ${}^3B_{1g}$  state should provide a good measure of the relative energies of these two MOs in  $(\text{CO})_6$ .

The UB3LYP and UCCSD(T) vertical IEs for removing an electron from each of these two orbitals in the  ${}^3B_{1g}$  state of  $(\text{CO})_6$  are given in Table 2. The vertical IEs were computed at the UB3LYP geometry of the triplet state from the energies of the triplet and of the radical cations formed from it. The adiabatic

**Table 1.** (U)B3LYP and (U)CCSD(T) Singlet–Triplet Energy Differences (kcal/mol) in  $(\text{CO})_n$ ,  $n = 2–6$ , at (U)B3LYP/6-311+G(2df)-Optimized  $D_{nh}$  Geometries<sup>a</sup>

	(U)B3LYP/6-311+G(2df)	(U)CCSD(T)/6-311+G(2df)
$(\text{CO})_2$	10.3 <sup>b</sup>	13.5 <sup>c</sup>
$(\text{CO})_3$	$-13.9^{d,e}$	$-26.5$
$(\text{CO})_4$	14.0 <sup>f</sup>	2.4
$(\text{CO})_5$	$-10.7^g$	$-27.0$
$(\text{CO})_6$	$-9.5$	$-27.8$

<sup>a</sup>A negative energy means that the singlet is calculated to be lower in energy than the triplet. <sup>b</sup>A broken symmetry density functional theory (BS-DFT) wave function was used for the singlet calculation, giving  $\langle S^2 \rangle = 1.0068$ . The value in the table was obtained by correcting the energy of the BS-DFT singlet for triplet spin contamination using the method of Yamaguchi et al. (Yamaguchi, K.; Jensen, F.; Dorigo, A.; Houk, K. N. *Chem. Phys. Lett.* **1988**, *149*, 537). <sup>c</sup>CCSD(T)/TZ2P//CCSD/DZP singlet-point energy using a single-determinant reference wave function.<sup>10k</sup> A value of 9.51 kcal/mol is obtained using a two-determinant reference wave function.<sup>10k</sup> <sup>d</sup>The  $D_{3h}$  geometry for singlet  $(\text{CO})_3$  with six  $\pi$  electrons has two imaginary frequencies. Following these modes leads to fragmentation to three CO molecules.<sup>36</sup> <sup>e</sup>The  $D_{3h}$  geometry for triplet  $(\text{CO})_3$  undergoes a Jahn–Teller distortion to a geometry with  $C_{2v}$  symmetry and one long C–C bond, lowering the energy by 27.1 kcal/mol. <sup>f</sup>Based on the energy of the singlet with eight  $\pi$  electrons.<sup>30</sup> <sup>g</sup>The  $D_{5h}$  geometry of triplet  $(\text{CO})_5$  undergoes a Jahn–Teller distortion to  $C_{2v}$  symmetry, lowering the energy by 2.2 kcal/mol.

IEs, computed using the UB3LYP-optimized geometries for the radical cations, are given in parentheses, next to the adiabatic IEs. Also given for comparison in Table 2 are the IEs computed for the  ${}^3B_{1u}$  state of  $(\text{CO})_4$ .<sup>12,38</sup>

Table 2 shows that the UB3LYP IE for removing an electron from the  $b_{2u}$   $\sigma$  MO of triplet  $(\text{CO})_6$  is calculated to be 19.5 (19.4) kcal/mol larger than the IE for removing an electron from the  $a_{2u}$   $\pi^*$  MO. The UCCSD(T) value for the IE difference between these two MOs is even larger, 25.7 (26.2) kcal/mol.

In contrast, as already discussed, in  $(\text{CO})_4$  the  $b_{2g}$   $\sigma$  MO has almost the same IE as the  $a_{2u}$   $\pi^*$  MO.<sup>12</sup> The difference in IEs is only  $-0.3$  (0.5) kcal/mol with UB3LYP and 2.8 (3.8) kcal/mol with UCCSD(T). The near degeneracy of these two MOs in  $(\text{CO})_4$  is, of course, the reason why, unlike the case in  $(\text{CO})_6$ ,  $(\text{CO})_4$  is predicted<sup>11b-d,12</sup> and found<sup>15</sup> to have a triplet ground state.

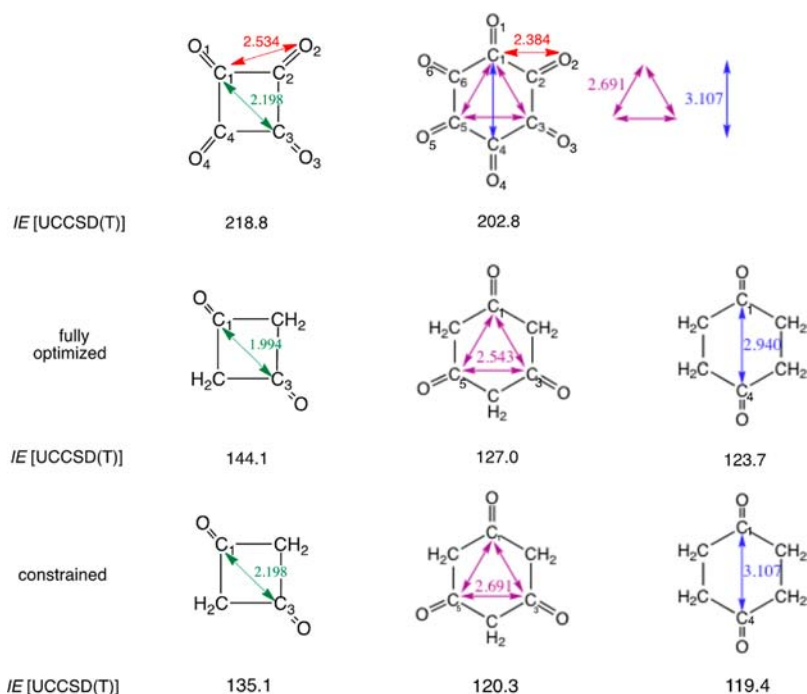
As shown in Table 2, an increase in the IE of the  $b_2$   $\sigma$  MO [ $b_{2g}$  in  $(\text{CO})_4$  and  $b_{2u}$  in  $(\text{CO})_6$ ] and a decrease in the IE of the  $a_{2u}$   $\pi^*$  MO both contribute to the much larger HOMO–LUMO energy difference in  $(\text{CO})_6$  than in  $(\text{CO})_4$ . At the UB3LYP level of theory the IE of the  $b_{2u}$  MO of  $(\text{CO})_6$  is 4.9 (5.7) kcal/mol lower in energy than that of the  $b_{2g}$  MO of  $(\text{CO})_4$ . At the UCCSD(T) level of theory, this difference in  $\sigma$  orbital IEs is slightly larger, amounting to 6.9 (8.8) kcal/mol.

Table 2 also shows that the IE of the  $a_{2u}$   $\pi^*$  orbital of  $(\text{CO})_6$  is higher than that of the  $a_{2u}$   $\pi^*$  orbital of  $(\text{CO})_4$  by 14.9 (13.2) kcal/mol with UB3LYP and by 16.0 (13.6) kcal/mol with UCCSD(T). Thus, on going from  $(\text{CO})_4$  to  $(\text{CO})_6$ , the increase in the IE of the  $a_{2u}$   $\pi^*$  MO is a factor of 2–3 larger than the decrease in the IE of the  $b_2$   $\sigma$  MO.

Why is the vertical IE of the  $a_{2u}$   $\pi^*$  MO of  $(\text{CO})_6$  15–16 kcal/mol higher than the IE of this MO in  $(\text{CO})_4$ ? One might first look for the reason in a difference between the bonded C–C or C–O distances. However, these distances (see the Supporting Information) are within 0.01 Å of each other in the triplet states of  $(\text{CO})_4$  and  $(\text{CO})_6$ , for which the IEs in Table 2 have been

**Table 2.** UB3LYP and UCCSD(T) Vertical and Adiabatic (in Parentheses) IEs (kcal/mol) of the Singly Occupied  $\sigma$  and  $\pi^*$  MOs in the Lowest Triplet States of Planar  $(\text{CO})_4^{12}$  and  $(\text{CO})_6$ , Computed at UB3LYP-Optimized Geometries with the 6-311+G(2df) Basis Set

molecule	UB3LYP		UCCSD(T)	
	IE( $\sigma$ )	IE( $\pi^*$ )	IE( $\sigma$ )	IE( $\pi^*$ )
$(\text{CO})_4$	230.7 (224.2)	231.0 (223.7)	221.6 (215.9)	218.8 (212.1)
$(\text{CO})_6$	235.6 (229.9)	216.1 (210.5)	228.5 (224.7)	202.8 (198.5)



**Figure 10.** Non-nearest-neighbor C–C and C–O distances (Å) and vertical IEs (kcal/mol) of the electron in the  $\pi^*$  MO in the lowest  $n \rightarrow \pi^*$  triplet states of cyclobutane-1,2,3,4-tetrone, cyclohexane-1,2,3,4,5,6-hexone, cyclobutane-1,3-dione, cyclohexane-1,3,5-trione, and cyclohexane-1,4-dione at planar geometries. For simplicity, only the UCCSD(T) IEs are given; the UB3LYP IEs are available in the Supporting Information. Differences between pairs of UB3LYP IEs are within about 2 kcal/mol of the corresponding differences between the UCCSD(T) IEs.

computed. Therefore, we must look elsewhere for a rationale, and at least two other contributors seem possible.

One is that, as shown in Figures 1, 2, and 9, these  $a_{2u} \pi^*$  MOs are C–O antibonding between every carbon–oxygen atom pair. The O–C–C bond angle determines how strong the antibonding interaction is between each 2p  $\pi$  oxygen AO and the pair of 2p  $\pi$  carbon AOs of the two carbonyl groups that are adjacent to it. As shown in Figure 10, the 135° O–C–C bond angle in  $(\text{CO})_4$  results in the C1–O2 distance being 2.534 Å, whereas the 120° O–C–C bond angle in  $(\text{CO})_6$  results in the C1–O2 distance being 2.384 Å. The 0.150 Å shorter C1–O2 distance in  $(\text{CO})_6$  than in  $(\text{CO})_4$  makes the antibonding interactions between the oxygen of one carbonyl group and the carbons of the two adjacent carbonyl groups more destabilizing to the  $a_{2u} \pi^*$  MO in  $(\text{CO})_6$  than in  $(\text{CO})_4$ .<sup>39</sup>

A second possible contributor to the higher IE of the  $a_{2u} \pi^*$  MO in triplet  $(\text{CO})_4$  than in triplet  $(\text{CO})_6$  is the difference between the sizes of the stabilizing 1,3 C–C interactions between the carbonyl carbons in these two compounds. As discussed in the section on  $(\text{CO})_4$ , the cross-ring  $\pi$  overlaps between the 2p  $\pi$  AOs on C1 and C3 and on C2 and C4 are bonding and stabilize the  $a_{2u} \pi^*$  MO of  $(\text{CO})_4$ . Of course, such 1,3  $\pi$  bonding interactions between 2p  $\pi$  AOs on carbon also exist in the  $a_{2u} \pi^*$  MO of  $(\text{CO})_6$ . In fact, as shown in Figure 10, each 2p  $\pi$  AO in  $(\text{CO})_6$

interacts with not one, but two 2p  $\pi$  AOs that are on next-nearest-neighbor carbons.

However, the C–C–C bond angles of 90° in  $(\text{CO})_4$ , compared to 120° in planar  $(\text{CO})_6$ , make the distance between next-nearest-neighbor carbons much smaller in  $(\text{CO})_4$  than in  $(\text{CO})_6$ . As shown in Figure 10, in the lowest triplet state the distance between C1 and C3 is 2.198 Å in  $(\text{CO})_4$ , compared to 2.691 Å in  $(\text{CO})_6$ , a difference of nearly 0.5 Å.<sup>40</sup> Although each carbon 2p  $\pi$  AO in  $(\text{CO})_6$  also interacts with a carbon 2p  $\pi$  AO directly across the six-membered ring, this 1,4 interaction occurs over an even larger distance of 3.107 Å.

We tested computationally whether the greater distances between C1 and C3 in  $(\text{CO})_6$  compared to  $(\text{CO})_4$  can account for the higher energy of the  $a_{2u} \pi^*$  MO in  $(\text{CO})_6$ . We calculated the vertical IEs of the  $\pi^*$  MOs in the lowest  $n \rightarrow \pi^*$  triplet states of cyclobutane-1,3-dione, cyclohexane-1,3,5-trione, and cyclohexane-1,4-dione. We performed our calculations at both partially optimized triplet geometries, in which the distances between the carbonyl carbons were constrained to be the same as those in  $(\text{CO})_4$  or in  $(\text{CO})_6$ , and at the fully optimized triplet geometries. The results of both sets of calculations are given in Figure 10.

As shown in Figure 10, in the lowest  $n \rightarrow \pi^*$  triplet state of cyclobutane-1,3-dione, with the C1–C3 distance constrained to be the same as that in  $(\text{CO})_4$ , the UCCSD(T) vertical IE of the



electron in the  $\pi^*$  MO is computed to be 135.1 kcal/mol. In the lowest  $n \rightarrow \pi^*$  triplet state of cyclohexane-1,3,5-trione, with the C1–C3, C1–C5, and C3–C5 bond distances constrained to be the same as those in  $(\text{CO})_6$ , the UCCSD(T) vertical IE of the electron in the  $\pi^*$  MO is 120.3 kcal/mol. The difference of 14.8 kcal/mol between these IEs is only slightly smaller than the 16.0 kcal/mol difference between the vertical UCCSD(T)  $\pi^*$  IEs of triplet  $(\text{CO})_4$  and triplet  $(\text{CO})_6$  in Table 2.

Figure 11, which depicts the lowest energy  $\pi^*$  MO of cyclobutane-1,3-dione and of cyclohexane-1,3,5-trione, shows



**Figure 11.** Lowest energy  $\pi^*$  MOs of cyclobutane-1,3-dione, cyclohexane-1,3,5-trione, and cyclohexane-1,4-dione.

that the difference between the IEs of these MOs is caused by more than just the effect of cross-ring interactions between the carbons of the carbonyl groups. Hyperconjugation, resulting from the interactions between the  $\pi^*$  orbitals of the carbonyl groups and the C–H bonding and C–H antibonding orbitals of the adjacent  $\text{CH}_2$  groups,<sup>41</sup> results in large contributions from  $\pi$ -type combinations of the  $\text{CH}_2$  hydrogens to the lowest energy  $\pi^*$  MOs of cyclobutane-1,3-dione and cyclohexane-1,3,5-trione. Comparison of Figure 11 with Figures 1, 2, and 9 shows that the hydrogen 1s AOs enter these two  $\pi^*$  orbitals with the same phasing as the oxygen 2p  $\pi$  AOs enter the  $a_{2u}$   $\pi^*$  MOs of  $(\text{CO})_4$  and  $(\text{CO})_6$ . Therefore, the difference between the IEs of the lowest  $\pi^*$  MOs of cyclobutane-1,3-dione and cyclohexane-1,3,5-trione contains a contribution that is very similar to that arising from the difference between the strengths of the O2–C1 antibonding interactions in the  $a_{2u}$   $\pi^*$  MOs of  $(\text{CO})_4$  and  $(\text{CO})_6$ .

As shown in Figure 10, the UCCSD(T) IE of the lowest energy  $\pi^*$  MO in fully optimized triplet cyclobutane-1,3-dione, with  $r(\text{C1–C3}) = 1.994 \text{ \AA}$ , is 9.0 kcal/mol higher than the IE of this MO in the geometry in which  $r(\text{C1–C3})$  is constrained to be 2.198  $\text{\AA}$ . Similarly, the UCCSD(T) IE of the lowest energy  $\pi^*$  MO in fully optimized triplet cyclohexane-1,3,5-trione, with  $r(\text{C1–C3}) = 2.543 \text{ \AA}$ , is 6.7 kcal/mol higher than the IE of this MO in the geometry in which  $r(\text{C1–C3})$  is constrained to be 2.691  $\text{\AA}$ . These results confirm that the IEs of these MOs do, in fact, increase as the C–C distances between the carbonyl carbons decrease.

The results in Figure 10 also reveal that the distance dependence of the  $\pi^*$  IEs is more than twice as large for a decrease in the C1–C3 distance from  $r = 2.198 \text{ \AA}$  to  $r = 1.994 \text{ \AA}$  ( $\Delta r = 0.204 \text{ \AA}$ ) in triplet cyclobutane-1,3-dione than for a decrease in the C1–C4 distance from  $r = 3.107 \text{ \AA}$  to  $r = 2.940 \text{ \AA}$  ( $\Delta r = 0.167 \text{ \AA}$ ) in triplet cyclohexane-1,4-dione. As would be expected for exponential changes in AO overlaps with distance, the smaller the distance between the interacting AOs of the carbonyl carbons, the more sensitive the  $\pi^*$  IE is to a change in this distance.

It seems surprising, however, that the UCCSD(T)  $\pi^*$  IE of triplet cyclohexane-1,3,5-trione at  $r(\text{C1–C3}) = 2.691 \text{ \AA}$  is only 0.9 kcal/mol larger than the UCCSD(T)  $\pi^*$  IE of triplet cyclohexane-1,4-dione at  $r(\text{C1–C4}) = 3.107 \text{ \AA}$ . In fact, the

UCCSD(T)  $\pi^*$  IE in triplet cyclohexane-1,3,5-trione at  $r(\text{C1–C3}) = 2.691 \text{ \AA}$  is actually 3.4 kcal/mol smaller than the UCCSD(T)  $\pi^*$  IE in triplet cyclohexane-1,4-dione at  $r(\text{C1–C4}) = 2.940 \text{ \AA}$ . If the  $\pi^*$  IEs increase with decreasing distance between the carbonyl groups, how can the relative values of these  $\pi^*$  IEs in the triplet trione and triplet dione be explained?

Inspection of Figure 11 provides the answer. This figure shows graphically that the carbonyl distance is not the only contributor to the difference between these IEs. Because each  $\text{CH}_2$  group in cyclohexane-1,3,5-trione hyperconjugates with not one, but two carbonyl groups, the hydrogens of the  $\text{CH}_2$  groups make a much larger contribution to the  $\pi^*$  MO of cyclohexane-1,3,5-trione than to the  $\pi^*$  MO of cyclohexane-1,4-dione. Therefore, the antibonding interactions between the  $\text{CH}_2$  hydrogens and the carbonyl carbons destabilize the  $\pi^*$  MO of cyclohexane-1,3,5-trione much more than the  $\pi^*$  MO of cyclohexane-1,4-dione. Consequently, as the bonding interactions between the carbonyl carbons in cyclohexane-1,3,5-trione decrease with increasing  $r(\text{C1–C3})$  distance, the antibonding interactions between the  $\text{CH}_2$  hydrogens and the carbonyl carbons result in the IE of the  $\pi^*$  MO of cyclohexane-1,3,5-trione becoming equal to or even less than the IE of the  $\pi^*$  MO of cyclohexane-1,4-dione.

Perhaps the most conclusive proof that the difference of 16.0 kcal/mol between the IEs of the  $a_{2u}$  MOs of triplet  $(\text{CO})_4$  and  $(\text{CO})_6$  is largely due to the shorter distance between C1 and C3 in triplet  $(\text{CO})_4$  than in triplet  $(\text{CO})_6$  comes from a calculation in which this distance between C1 and C4 in triplet cyclohexane-1,4-dione was fixed at 1.994  $\text{\AA}$ , the same as the distance between C1 and C3 in fully optimized, triplet cyclobutane-1,3-dione. The computed vertical UCCSD(T) IE of triplet cyclohexane-1,4-dione, thus constrained, is 154.3 kcal/mol, which is an increase of 34.9 kcal/mol over the vertical IE of 119.4 kcal/mol in triplet cyclohexane-1,4-dione, with the C1–C4 distance constrained to be 3.107  $\text{\AA}$ .<sup>42</sup>

This result, combined with the results given in Figure 10, provides excellent evidence that the higher energy (lower IE) of the  $a_{2u}$   $\pi^*$  MO in  $(\text{CO})_6$  compared to  $(\text{CO})_4$  can be attributed to a combination of the weaker C1–C3 bonding interactions and the stronger non-neighbor C1–O2 antibonding interactions in the  $a_{2u}$   $\pi^*$  MO of  $(\text{CO})_6$ . As already noted, the difference between the orbital energies of the  $a_{2u}$   $\pi^*$  MOs of these two molecules is the chief reason<sup>40</sup> that  $(\text{CO})_4$  has a triplet ground state,<sup>11,12,15</sup> whereas  $(\text{CO})_6$  is both calculated and found<sup>34</sup> to have a singlet ground state.

## SUMMARY AND CONCLUSIONS

The simplest answer to the question, posed in the title, of why  $(\text{CO})_4$  has a triplet ground state is that its electronic structure resembles that of  $(\text{CO})_2$ . In both  $(\text{CO})_{2n}$  molecules a pair of electrons are removed from, what are in  $2n$  CO molecules, an antibonding combination of carbon lone-pair orbitals and distributed between symmetric combinations of CO  $\pi^*$  orbitals that lie in orthogonal planes. In  $(\text{CO})_2$  the  $\pi^*$  orbitals are degenerate by symmetry,<sup>10</sup> and since these MOs are not disjoint,<sup>13</sup> Hund's rule<sup>14</sup> should apply. Therefore, the ground state of  $(\text{CO})_2$  can unequivocally be predicted to be a triplet, without performing any electronic structure calculations.

In contrast, the C–C bonding combinations of the  $\pi^*$  orbitals of four CO molecules become the  $b_{2g}$   $\sigma$  and the  $a_{2u}$   $\pi$  MO of  $(\text{CO})_4$ . These orbitals are not degenerate by symmetry, so performing electronic structure calculations is necessary to predict the ground state of  $(\text{CO})_4$ . For such a small molecule, performing calculations at a high enough level to order the electronic states

correctly has proven to be surprisingly challenging,<sup>11</sup> but the best available calculations predict the triplet to be the ground state by ca. 2 kcal/mol.

A more qualitative, but possibly more convincing, argument for a triplet ground state in  $(\text{CO})_4$  comes from calculations which show the  $b_{2g}$   $\sigma$  and the  $a_{2u}$   $\pi$  MOs of  $(\text{CO})_4$  to have nearly the same energies.<sup>12</sup> Then Hund's rule can again be used to predict a triplet ground state for  $(\text{CO})_4$ <sup>14</sup>—a prediction which has been confirmed experimentally.<sup>15</sup>

The near degeneracy of the  $b_{2g}$   $\sigma$  MO and the  $a_{2u}$   $\pi$  MO of  $(\text{CO})_4$  is, at first, surprising, because C–C  $\sigma$  bonds are usually stronger than C–C  $\pi$  bonds. However, the  $b_{2g}$   $\sigma$  orbital of  $(\text{CO})_4$  is antibonding between C1 and C3 and between C2 and C4, whereas the  $a_{2u}$   $\pi$  MO is bonding between these pairs of carbons. These cross-ring interactions result in the near degeneracy of the  $b_{2g}$   $\sigma$  MO and the  $a_{2u}$   $\pi$  MO of  $(\text{CO})_4$ .

Not only in  $(\text{CO})_2$  and in  $(\text{CO})_4$ , but in  $(\text{CO})_{2n}$  molecules in general, a pair of electrons must be removed from a  $b_{1g}$  ( $b_{1g}$  if  $n$  is even and  $b_{1u}$  if  $n$  is odd) combination of carbon lone-pair orbitals and distributed between a  $b_2$  ( $b_{2g}$  if  $n$  is even and  $b_{2u}$  if  $n$  is odd)  $\sigma$  MO and an  $a_{2u}$   $\pi$  MO. However, our calculations find that, in agreement with experiment,<sup>34</sup>  $(\text{CO})_6$  has a singlet ground state, in which the  $b_{2u}$   $\sigma$  MO is doubly occupied.

There are several reasons for the difference between the spins of the ground states of  $(\text{CO})_4$  and  $(\text{CO})_6$ . The 30° larger internal C–C–C bond angles in  $(\text{CO})_6$  than in  $(\text{CO})_4$  make the size of the C1–C3 bonding interactions in the  $a_{2u}$   $\pi$  MO and the C1–C3 antibonding interactions in the  $b_2$   $\sigma$  MO<sup>40</sup> smaller in  $(\text{CO})_6$  than in  $(\text{CO})_4$ . The first of these changes raises the energy of the  $a_{2u}$   $\pi$  MO of  $(\text{CO})_6$  relative to the energy of this MO in  $(\text{CO})_4$ , and the second effect lowers the energy of the  $b_{2u}$   $\sigma$  MO of  $(\text{CO})_6$  relative to the energy of the  $b_{2g}$  MO of  $(\text{CO})_4$ . Both of these changes serve to stabilize the  $b_2$   $\sigma$  MO relative to the  $a_{2u}$   $\pi$  MO in  $(\text{CO})_6$  compared to  $(\text{CO})_4$ .

The 15° smaller O–C–C external angles in  $(\text{CO})_6$  than in  $(\text{CO})_4$  increase the size of the C1–O2 (and, of course, the C3–O2) antibonding  $\pi$  interactions in  $(\text{CO})_6$  compared to  $(\text{CO})_4$ . The resulting destabilization of the  $a_{2u}$   $\pi$  MO of  $(\text{CO})_6$  further increases the energy difference between the  $b_{2u}$   $\sigma$  MO and the  $a_{2u}$   $\pi$  MO of  $(\text{CO})_6$  and thus stabilizes the lowest singlet state of  $(\text{CO})_6$  relative to the triplet state.

Like  $(\text{CO})_6$ , all the members of the  $(\text{CO})_{2n+1}$  series of oxocarbons are predicted to have singlet ground states. This prediction has been confirmed for  $(\text{CO})_5$ .<sup>34</sup> However, the reason why the members of the  $(\text{CO})_{2n+1}$  series have singlet ground states is rather different from the reason that  $(\text{CO})_6$  is calculated and found<sup>34</sup> to have a singlet ground state.

In forming  $(\text{CO})_{2n+1}$  from  $2n + 1$  CO molecules, the degenerate pairs of empty, in-plane,  $\pi^*$  MOs mix with and stabilize the degenerate pairs of filled carbon lone-pair MOs. Consequently, unlike the case in forming  $(\text{CO})_{2n}$  from  $2n$  CO molecules, there is no crossing between filled and empty MOs in forming  $(\text{CO})_{2n+1}$  from  $2n + 1$  CO molecules. Therefore,  $(\text{CO})_{2n+1}$  molecules have closed shells of  $\sigma$  electrons and substantial energy differences between the degenerate pair of  $e_n$ ,  $\sigma$  HOMOs and the  $a_2''$ ,  $\pi$  LUMO.

The smooth correlation between the filled orbitals of the reactant and product means that, unlike the case in the fragmentation of  $(\text{CO})_{2n}$  molecules to  $2n$  molecules of CO, concerted bond breaking is allowed by orbital symmetry in the fragmentation of  $(\text{CO})_{2n+1}$  to  $2n + 1$  CO molecules. This is one of the reasons that concerted fragmentation of  $(\text{CO})_3$  has a negligible barrier.

However, in the fragmentation of  $(\text{CO})_5$  to five CO molecules, not only is the  $D_{3h}$  energy maximum 55.7 kcal/mol above that of the reactant, but this structure has two degenerate pairs of vibrations with imaginary frequencies. Therefore, although the fragmentation of  $(\text{CO})_5$  to five CO molecules is allowed to be concerted by orbital symmetry,<sup>22</sup> pathways involving stepwise bond breaking are apparently preferred.

In the fragmentation of  $(\text{CO})_{2n}$  to  $2n$  CO molecules there is a crossing between filled and empty MOs of the reactant and product. Therefore, concerted fragmentation is forbidden by orbital symmetry,<sup>22</sup> so the C–C bonds break in a stepwise fashion. We have confirmed that this is the case for the fragmentation of  $(\text{CO})_4$  to four CO molecules.<sup>27</sup>

In summary,  $(\text{CO})_{2n+1}$  oxocarbons are all predicted to have singlet ground states. In the  $(\text{CO})_{2n}$  series only  $(\text{CO})_2$  and  $(\text{CO})_4$  are predicted to have triplet ground states. The ground state of  $(\text{CO})_6$  is a singlet, because the 1,3 bonding and antibonding interactions, which lead to the  $b_{2g}$   $\sigma$  and  $a_{2u}$   $\pi$  MOs of  $(\text{CO})_4$  having nearly the same energy, are attenuated by the larger C–C–C bond angles and the smaller O–C–C bond angles in  $(\text{CO})_6$ . The substantial energy gap between the  $b_{2u}$   $\sigma$  and  $a_{2u}$   $\pi$  orbitals in  $(\text{CO})_6$  that results is the reason why this oxocarbon is predicted and found<sup>34</sup> to have a singlet ground state.

## ■ ASSOCIATED CONTENT

### ● Supporting Information

Nonconcerted fragmentation pathways for  $(\text{CO})_4$ , structural and energetic analysis for five conformers of  $(\text{CO})_6$ , UB3LYP vertical IEs of the electron in the  $\pi^*$  MO in the lowest  $n \rightarrow \pi^*$  triplet states of  $(\text{CO})_4$ ,  $(\text{CO})_6$ , cyclobutane-1,3-dione ( $\text{C}_4\text{H}_4\text{O}_2$ ), cyclohexane-1,3,5-trione ( $\text{C}_6\text{H}_6\text{O}_3$ ), and cyclohexane-1,4-dione ( $\text{C}_6\text{H}_6\text{O}_2$ ) at planar geometries, and all of the optimized geometries and energies for (a) the lowest singlet and triplet states of  $(\text{CO})_n$ ,  $n = 2-6$ , (b) the radical cations of  $(\text{CO})_4$  and  $(\text{CO})_6$ , and (c) the  $n \rightarrow \pi^*$  triplet states and radical cations of planar  $\text{C}_4\text{H}_4\text{O}_2$ ,  $\text{C}_6\text{H}_6\text{O}_2$ , and  $\text{C}_6\text{H}_6\text{O}_3$ . This material is available free of charge via the Internet at <http://pubs.acs.org>.

## ■ AUTHOR INFORMATION

### Corresponding Author

[rh34@cornell.edu](mailto:rh34@cornell.edu); [borden@unt.edu](mailto:borden@unt.edu)

### Notes

The authors declare no competing financial interest.

## ■ ACKNOWLEDGMENTS

We thank Dr. X.-B. Wang for communicating to us his unpublished results on the negative ion photoelectron spectra of  $(\text{CO})_5^{\bullet-}$  and  $(\text{CO})_6^{\bullet-}$ . This research was supported by generous grants from the National Science Foundation to R.H. and W.T.B. and by Grant B0027 from the Robert A. Welch Foundation to W.T.B.

## ■ REFERENCES

- (1) For a review, see: Seitz, G.; Imming, P. *Chem. Rev.* **1992**, *92*, 1227.
- (2) Weiss, E.; Büchner, W. *Helv. Chim. Acta* **1963**, *46*, 1121.
- (3) (a) Eggerding, D.; West, R. *J. Am. Chem. Soc.* **1975**, *97*, 207.
- (b) Eggerding, D.; West, R. *J. Am. Chem. Soc.* **1976**, *98*, 3641.
- (4) Cohen, S.; Lacher, J. R.; Park, J. D. *J. Am. Chem. Soc.* **1959**, *81*, 3480.
- (5) Gmelin, L. *Ann. Phys. (Leipzig)* **1825**, *4*, 31.
- (6) Heller, J. F. *Justus Liebigs Ann. Chem.* **1837**, *24*, 1.
- (7) For a review see: (a) West, R. *Oxocarbons*; Academic Press: New York, 1980. Recent papers include the following: (b) Schleyer, P. v. R.;

- Najafian, K.; Kiran, B.; Jiao, H. *J. Org. Chem.* **2000**, *65*, 426 and references therein. (c) Jiao, H.; Wu, H.-S. *J. Org. Chem.* **2003**, *68*, 1475. (d) Summerscales, O. T.; Cloke, F. G. N.; Hitchcock, P. B.; Green, J. C.; Hazari, N. *Science* **2006**, *311*, 829. (e) Summerscales, O. T.; Cloke, F. G. N.; Hitchcock, P. B.; Green, J. C.; Hazari, N. *J. Am. Chem. Soc.* **2006**, *128*, 9602. (f) Frey, A. S.; Cloke, F. G. N.; Hitchcock, P. B.; Day, I. J.; Green, J. C.; Aitken, G. *J. Am. Chem. Soc.* **2008**, *130*, 13816. (g) Junqueira, G. M. A.; Rocha, W. R.; De Almeida, W. B.; Dos Santos, H. F. *Phys. Chem. Chem. Phys.* **2002**, *4*, 2517. (h) Wyrwas, R. B.; Jarrold, C. C. *J. Am. Chem. Soc.* **2006**, *128*, 13688. (i) Arthur, T. B.; Peschke, M.; Kebarle, P. *Int. J. Mass Spectrom.* **2003**, *228*, 1017. (j) Chen, H.; Armand, M.; Courty, M.; Jiang, M.; Grey, C. P.; Dolhem, F.; Tarascon, J.-M.; Poizot, P. *J. Am. Chem. Soc.* **2009**, *131*, 8984.
- (8) (a) Schröder, D.; Schwarz, H.; Dua, S.; Blanksby, S. I.; Bowie, J. H. *Int. J. Mass Spectrom.* **1999**, *188*, 17. (b) Hsu, D. S. Y.; Lin, M. C. *J. Chem. Phys.* **1978**, *68*, 4347. (c) For a review of vicinal polycarbonyl compounds, see: Rubin, M. B.; Gleiter, R. *Chem. Rev.* **2000**, *100*, 1121.
- (9) (a) Farnell, L.; Radom, L.; Vincent, M. A. *J. Mol. Struct.* **1981**, *76*, 1. (b) Sabzyan, H.; Noorbala, M. R. *J. Mol. Struct.* **2003**, *626*, 143. (c) Corkran, G.; Ball, D. W. *J. Mol. Struct.* **2004**, *668*, 171. (d) Sahu, P. K.; Lee, S.-L. *Int. J. Quantum Chem.* **2005**, *103*, 314. (e) Nazari, F. *J. Mol. Struct.* **2006**, *760*, 29.
- (10) (a) Hirst, D. M.; Hopton, J. D.; Linnett, J. W. *Tetrahedron Suppl.* **1963**, *2*, 15. (b) Glmarc, B. M. *J. Am. Chem. Soc.* **1970**, *92*, 266. (c) Bodor, N.; Dewar, M. J. S.; Harget, A.; Haselbach, E. *J. Am. Chem. Soc.* **1970**, *92*, 3854. (d) Haddon, R. C. *Tetrahedron Lett.* **1972**, *13*, 3897. (e) Fleischhauer, J.; Beckers, M.; Scharf, H.-D. *Tetrahedron Lett.* **1973**, *14*, 4275. (f) Beebe, N. H. F.; Sabin, J. R. *Chem. Phys. Lett.* **1974**, *24*, 389. (g) Haddon, R. C.; Poppinger, D.; Radom, L. *J. Am. Chem. Soc.* **1975**, *97*, 1645. (h) Raine, G. P.; Schaefer, H. F., III; Haddon, R. C. *J. Am. Chem. Soc.* **1983**, *105*, 194. (i) Frenking, G. *Angew. Chem., Int. Ed. Engl.* **1990**, *29*, 1410. (j) Janoschek, R. *J. Mol. Struct.* **1991**, *232*, 147. (k) Korkin, A. A.; Balkova, A.; Bartlett, R. J.; Boyd, R. J.; Schleyer, P. v. R. *J. Phys. Chem.* **1996**, *100*, 5702. (l) Schröder, D.; Heinemann, C.; Schwarz, H.; Harvey, J. N.; Dua, S.; Blanksby, S. J.; Bowie, J. H. *Chem.—Eur. J.* **1998**, *4*, 2550. (m) Talbi, D.; Chandler, G. S. *J. Phys. Chem. A* **2000**, *104*, 5872. (n) Wang, H.-Y.; Lu, X.; Huang, R.-B.; Zheng, L.-S. *J. Mol. Struct.* **2002**, *593*, 187. (o) Trindle, C. *Int. J. Quantum Chem.* **2003**, *93*, 286. (p) Maclagan, R. G. A. R. *J. Mol. Struct.* **2005**, *713*, 107. (q) Golovin, A. V.; Ponomarev, D. A.; Takhistov, V. V. *J. Comput. Method. Mol. Des.* **2011**, *1*, 14. (r) Domene, C.; Fowler, P. W.; Jennessens, L. W.; Steiner, E. *Chem.—Eur. J.* **2007**, *13*, 269.
- (11) (a) Gleiter, R.; Hyla-Kryspin, I.; Pfeifer, K.-H. *J. Org. Chem.* **1995**, *60*, 5878. (b) Jiao, H.; Frapper, G.; Halet, J.-F.; Saillard, J.-Y. *J. Phys. Chem. A* **2001**, *105*, 5945. (c) Zhou, X.; Hrovat, D. A.; Gleiter, R.; Borden, W. T. *Mol. Phys.* **2009**, *107*, 863. (d) Hansen, J. A.; Bauman, N. P.; Levine, B.; Borden, W. T.; Piecuch, P. Manuscript in preparation.
- (12) Zhou, X.; Hrovat, D. A.; Borden, W. T. *J. Phys. Chem. A* **2010**, *114*, 1304.
- (13) (a) Davidson, E. R.; Borden, W. T. *J. Am. Chem. Soc.* **1977**, *99*, 2053. (b) Review: Borden, W. T. In *Diradicals*; Borden, W. T., Ed.; Wiley-Interscience: New York, 1982; pp 1–72.
- (14) Reviews: (a) Borden, W. T.; Iwamura, H.; Berson, J. A. *Acc. Chem. Res.* **1994**, *27*, 109. (b) Kutzelnigg, W. *Angew. Chem., Int. Ed. Engl.* **1996**, *35*, 572. (c) Hrovat, D. A.; Borden, W. T. *THEOCHEM* **1997**, *398*, 211. (d) Hrovat, D. A.; Borden, W. T. In *Modern Electronic Structure Theory and Applications in Organic Chemistry*; Davidson, E. R., Ed.; World Scientific Publishing Co.: Singapore, 1997; pp 171–195.
- (15) Guo, J.-C.; Hou, G.-L.; Li, S. D.; Wang, X.-B. *J. Phys. Chem. Lett.* **2012**, *3*, 304.
- (16) B3LYP is a combination of Becke's three-parameter hybrid exchange functional (B3)<sup>17</sup> with the electron correlation functional of Lee, Yang, and Parr (LYP).<sup>18</sup>
- (17) Becke, A. D. *J. Chem. Phys.* **1993**, *98*, 5648.
- (18) Lee, C.; Yang, W.; Parr, R. G. *Phys. Rev. B* **1988**, *37*, 785.
- (19) (a) Purvis, G. D.; Bartlett, R. J. *J. Chem. Phys.* **1982**, *76*, 1910. (b) Raghavachari, K.; Trucks, G. W.; Pople, J. A.; Head-Gordon, M. H. *Chem. Phys. Lett.* **1989**, *157*, 479.
- (20) Krishnan, R.; Binkely, J. S.; Seeger, R.; Pople, J. A. *J. Chem. Phys.* **1980**, *72*, 650.
- (21) Frisch, M. J.; Trucks, G. W.; Schlegel, H. B.; Scuseria, G. E.; Robb, M. A.; Cheeseman, J. R.; Scalmani, G.; Barone, V.; Mennucci, B.; Petersson, G. A.; Nakatsuji, H.; Caricato, M.; Li, X.; Hratchian, H. P.; Izmaylov, A. F.; Bloino, J.; Zheng, G.; Sonnenberg, J. L.; Hada, M.; Ehara, M.; Toyota, K.; Fukuda, R.; Hasegawa, J.; Ishida, M.; Nakajima, T.; Honda, Y.; Kitao, O.; Nakai, H.; Vreven, T.; Montgomery Jr. J. A.; Peralta, J. E.; Ogliaro, F.; Bearpark, M.; Heyd, J. J.; Brothers, E.; Kudin, K. N.; Staroverov, V. N.; Kobayashi, R.; Normand, J.; Raghavachari, K.; Rendell, A.; Burant, J. C.; Iyengar, S. S.; Tomasi, J.; Cossi, M.; Rega, N.; Millam, N. J.; Klene, M.; Knox, J. E.; Cross, J. B.; Bakken, V.; Adamo, C.; Jaramillo, J.; Gomperts, R.; Stratmann, R. E.; Yazyev, O.; Austin, A. J.; Cammi, R.; Pomelli, C.; Ochterski, J. W.; Martin, R. L.; Morokuma, K.; Zakrzewski, V. G.; Voth, G. A.; Salvador, P.; Dannenberg, J. J.; Dapprich, S.; Daniels, A. D.; Farkas, O.; Foresman, J. B.; Ortiz, J. V.; Cioslowski, J.; Fox, D. J. *Gaussian 09*, revision A.02; Gaussian, Inc.: Wallingford, CT, 2009.
- (22) Woodward, R. B.; Hoffmann, R. *Angew. Chem., Int. Ed. Engl.* **1969**, *8*, 781.
- (23) The active space for the CASSCF calculations on the concerted fragmentation of (CO)<sub>4</sub> to four CO molecules consisted of the four C–C,  $\sigma$  bonding MOs of (CO)<sub>4</sub> and their four antibonding counterparts.
- (24) (a) Anderson, K.; Malmqvist, P. A.; Roos, B. O. *J. Chem. Phys.* **1992**, *96*, 1218. (b) Anderson, K.; Malmqvist, P. A.; Roos, B. O.; Sadlej, A. J.; Wolinski, K. *J. Chem. Phys.* **1990**, *94*, 5483.
- (25) The CASSCF and CASPT2 calculations were performed using MOLCAS: Karlström, G.; Lindh, R.; Malmqvist, P. Å.; Roos, B. O.; Ryde, U.; Veryazov, V. V.; Widmark, P.-O.; Cossi, M.; Schimmelpfennig, B.; Neogrady, P.; Seijo, L. *Comput. Mater. Sci.* **2003**, *28*, 222.
- (26) As is conventional, energy differences in this paper are reported to the nearest 0.1 kcal/mol. However, the difference of 16 kcal/mol between the CASSCF and CASPT2 exothermicities of the fragmentation reaction makes it clear that at least the former value is probably not accurate to even 10 kcal/mol.
- (27) For example, breaking of two adjacent C–C bonds would lead to one molecule each of (CO)<sub>3</sub> and CO, and the (CO)<sub>3</sub> fragment would then be expected to decompose to three CO molecules, with little or no barrier. We have, in fact, computed the energy for this mode of stepwise fragmentation of (CO)<sub>4</sub>, but because the stepwise fragmentation of (CO)<sub>4</sub> is not really germane to the central theme of this paper, we have relegated the results of these calculations to the Supporting Information.
- (28) Jorgensen, W. L.; Salem, L. *The Organic Chemist's Book of Orbitals*; Academic Press: New York, 1973.
- (29) Nevertheless, the presence of a low-lying, empty, a<sub>2</sub><sup>u</sup> MO in (CO)<sub>3</sub> and in other (CO)<sub>2n+1</sub> molecules and of a low-lying, empty, a<sub>2u</sub> MO in the closed-shell singlet states of (CO)<sub>2</sub>, (CO)<sub>4</sub>, and other (CO)<sub>2n</sub> molecules is the reason for the stability of the (CO)<sub>n</sub><sup>-2</sup> dianions.<sup>7</sup>
- (30) The lowest singlet state of (CO)<sub>4</sub> is actually computed by UB3LYP to be the open-shell, <sup>1</sup>B<sub>2u</sub> state, which has the same orbital occupancy as the triplet ground state.<sup>11b,c</sup> After correction of the UB3LYP energy of the mixed ( $\langle S^2 \rangle = 1.017$ ) <sup>1</sup>B<sub>2u</sub>/<sup>3</sup>B<sub>2u</sub> state for spin contamination, the open-shell, <sup>1</sup>B<sub>2u</sub> state lies lower in energy than the closed-shell, <sup>1</sup>A<sub>1g</sub> state with eight  $\pi$  electrons by 9.7 kcal/mol at the UB3LYP/6-311+G(2df) level of theory. After correction of the UCCSD(T) energy of the mixed ( $\langle S^2 \rangle = 1.141$ ) <sup>1</sup>B<sub>2u</sub>/<sup>3</sup>B<sub>2u</sub> state for spin contamination in the UHF reference wave function, (U) CCSD(T)/6-311+G(2df) calculations place <sup>1</sup>B<sub>2u</sub> 3.2 kcal/mol above the <sup>1</sup>A<sub>1g</sub> state with eight  $\pi$  electrons. The <sup>1</sup>A<sub>1g</sub> state with 10  $\pi$  electrons is computed to be 4.1 kcal/mol lower and 3.4 kcal/mol higher in energy than the <sup>1</sup>A<sub>1g</sub> state with 8  $\pi$  electrons by, respectively, B3LYP and CCSD(T) calculations.
- (31) The two vibrations of D<sub>3h</sub> (CO)<sub>3</sub> with imaginary frequencies are of e<sup>u</sup> symmetry. Therefore, these vibrations not only involve shortening of some C–C bonds and lengthening of others but also symmetry breaking motions of the oxygen atoms of the carbonyl groups out of the plane of the three carbons. These e<sup>u</sup> vibrations have the correct symmetry to allow the high-lying, filled e<sup>u</sup>  $\sigma$  MOs of (CO)<sub>3</sub> to mix with the low-lying empty a<sub>2</sub><sup>u</sup>  $\pi$  MO. The barrierless fragmentation of singlet

(CO)<sub>3</sub> at the B3LYP level<sup>7b,9</sup> can be attributed, in part, to this orbital mixing in a second-order Jahn–Teller effect.<sup>32</sup>

(32) (a) Öpik, U.; Pryce, M. H. L. *Proc. R. Soc. London, A* **1957**, *238*, 425. (b) Bader, R. F. W. *Can. J. Chem.* **1962**, *40*, 1164. (c) Pearson, R. G. *J. Am. Chem. Soc.* **1969**, *91*, 4947.

(33) Zimmerman, H. E. *Acc. Chem. Res.* **1971**, *4*, 272.

(34) Wang, X.-B. Private communication.

(35) It may well be that, for larger rings and for an infinite chain or ring, more than one in-plane  $\pi^*$  MO is occupied and more than one lone-pair combination is vacated. In band theory language, the miniband from the lone pairs may overlap the miniband formed from the in-plane  $\pi^*$  orbitals.

(36) In contrast, a C<sub>2v</sub> geometry with one long C–C bond is a B3LYP local minimum for the singlet state of (CO)<sub>3</sub> that has eight  $\pi$  electrons.

(37) Koopmans, T. *Physica* **1934**, *1*, 104.

(38) We have also computed the UB3LYP/6-311+G(2df) EAs for forming the triplet state of (CO)<sub>4</sub> and (CO)<sub>6</sub> from the <sup>2</sup>A<sub>2u</sub> and <sup>2</sup>B<sub>2</sub> radical anions. The calculations show that the larger size of (CO)<sub>6</sub> compared to (CO)<sub>4</sub> selectively stabilizes both the <sup>2</sup>A<sub>2u</sub> and <sup>2</sup>B<sub>2</sub> radical anions of (CO)<sub>6</sub> relative to those of (CO)<sub>4</sub> by about 24 kcal/mol. Thus, the adiabatic IEs of electrons in the  $\sigma$  MOs of the <sup>2</sup>A<sub>2u</sub> radical anions of (CO)<sub>6</sub> (EA = 108.6) and (CO)<sub>4</sub> (EA = 78.6),<sup>12</sup> in forming the triplet states of the neutrals, differ by 30.0 kcal/mol. This is 24.3 kcal/mol more than the difference between the adiabatic IEs of electrons in the  $\sigma$  MOs of the triplet states of (CO)<sub>6</sub> and (CO)<sub>4</sub> in Table 2. Similarly, the adiabatic IEs of electrons in the  $\pi^*$  MO of the <sup>2</sup>B<sub>2u</sub> radical anion of (CO)<sub>6</sub> (EA = 92.0 kcal/mol) and in the  $\pi^*$  MO of the <sup>2</sup>B<sub>2g</sub> radical anion of (CO)<sub>4</sub> (EA = 81.3 kcal/mol),<sup>12</sup> in forming the triplet states of the neutrals, differ by 10.7 kcal/mol. This is 23.9 kcal/mol more than the difference between the IEs of electrons in the  $\sigma$  MOs of the triplet states of (CO)<sub>6</sub> and (CO)<sub>4</sub> in Table 2.

(39) As shown in Figures 1, 2, and 9, the interaction between the 2p  $\pi$  AOs on adjacent oxygens is bonding in (CO)<sub>6</sub> and in (CO)<sub>4</sub>. Since the distances between adjacent oxygens of  $r(\text{O1–O2}) = 2.774 \text{ \AA}$  in (CO)<sub>6</sub> are 0.456  $\text{\AA}$  smaller than those of  $r(\text{O1–O2}) = 3.230 \text{ \AA}$  in (CO)<sub>4</sub>, O1–O2  $\pi$  bonding interactions act to stabilize the a<sub>2u</sub> MO more in (CO)<sub>6</sub> than in (CO)<sub>4</sub>. However, there are twice as many antibonding interactions involving each 2p  $\pi$  oxygen AO and the pair of 2p  $\pi$  carbon AOs of the two carbonyl groups that are adjacent to it than there are O1–O2 bonding interactions. Moreover, these C1–O2 antibonding  $\pi$  interactions involve considerably shorter distances [ $r(\text{C1–O2}) = 2.384 \text{ \AA}$  in (CO)<sub>6</sub> and  $r(\text{C1–O2}) = 2.534 \text{ \AA}$  in (CO)<sub>4</sub>] than the O1–O2 bonding interactions. Therefore, C1–O2 antibonding interactions destabilize the a<sub>2u</sub>  $\pi$  MOs of both (CO)<sub>6</sub> and (CO)<sub>4</sub> considerably more than the O1–O2 bonding interactions stabilize these MOs.

(40) As shown in Figures 1 and 2, in the b<sub>2g</sub>  $\sigma$  MO of (CO)<sub>4</sub> the interaction between the 2p AOs at C1 and C3 is antibonding. Figure 9 shows that this is also the case in the b<sub>2u</sub>  $\sigma$  MO of (CO)<sub>6</sub>. However, the 0.5  $\text{\AA}$  greater distance between C1 and C3 in (CO)<sub>6</sub> than in (CO)<sub>4</sub> should stabilize the b<sub>2u</sub>  $\sigma$  MO of (CO)<sub>6</sub> relative to the b<sub>2g</sub>  $\sigma$  MO of (CO)<sub>4</sub>. Although there are certainly many contributors to the 5–7 kcal/mol difference between the IEs of these two MOs in Table 2, one factor that makes the IE of the b<sub>2u</sub> MO of (CO)<sub>6</sub> larger than the IE of the b<sub>2g</sub> MO of (CO)<sub>4</sub> is certainly the greater distance between C1 and C3 in (CO)<sub>6</sub> than in (CO)<sub>4</sub>.

(41) The  $\pi^*$  orbitals mix in an antibonding way with the C–H  $\sigma$  orbitals, but in a bonding way with the C–H  $\sigma^*$  orbitals. This mixing of  $\pi^*$  with both  $\sigma$  and  $\sigma^*$  C–H orbitals results in the near cancellation of the contributions from the CH<sub>2</sub> carbons to the resulting  $\pi^*$  MOs, but additive contributions from the CH<sub>2</sub> hydrogens.

(42) With the distance between C1 and C4 in triplet cyclohexane-1,4-dione constrained to be 1.994  $\text{\AA}$ , the UCCSD(T) vertical IE of 154.3 kcal/mol for the lowest  $\pi^*$  MO is 10.2 kcal/mol larger than the IE of the lowest  $\pi^*$  MO in fully optimized 1,3-cyclobutanedione, with the same distance between the carbonyl carbons. The reason for this result can again be seen in Figure 11. The interactions between the carbonyl carbons and the four pairs of C–H bonds in the lowest  $\pi^*$  MO of cyclohexane-1,4-dione are less destabilizing than the interactions

between the carbonyl carbons and the two pairs of C–H bonds in the lowest  $\pi^*$  MO cyclobutane-1,3-dione.